

# Simultaneous Determination of Folic Acid and Uric Acid under Coexistence of L-Ascorbic Acid Using a Modified Electrode Based on Poly(3,4-Ethylenedioxythiophene) and Functionalized Single-Walled Carbon Nanotubes Composite

Tao Nie<sup>1,2,†</sup>, Limin Lu<sup>1,2,†</sup>, Ling Bai<sup>1,\*</sup>, Jingkun Xu<sup>2,\*</sup>, Kaixin Zhang<sup>2</sup>,  
Ouzhang<sup>2</sup>, Yangping Wen<sup>1,2</sup>, Liping Wu<sup>2</sup>

<sup>1</sup>College of Science, Jiangxi Agricultural University, Nanchang 330045, PR China

<sup>2</sup>Jiangxi Key Laboratory of Organic Chemistry, Jiangxi Science and Technology Normal University, Nanchang 330013, PR China

†These authors contributed equally to this work and should be considered co-first authors.

\*E-mail: [bailing716@yahoo.com.cn](mailto:bailing716@yahoo.com.cn); [xujingkun@tsinghua.org.cn](mailto:xujingkun@tsinghua.org.cn)

Received: 28 March 2013 / Accepted: 18 April 2013 / Published: 1 May 2013

---

In this study, a highly sensitive and selective sensor based on poly(3,4-ethylenedioxythiophene) (PEDOT) and  $\beta$ -cyclodextrin functionalized single-walled carbon nanotubes ( $\beta$ -CD-SWCNT) composite was fabricated for the simultaneous determination of folic acid (FA) and uric acid (UA) under coexistence of ascorbic acid (AA). The modified electrode combined the features of PEDOT and SWCNT, which hold excellent conductivity, low cost and high surface areas for working as an efficient electron-mediator for FA and UA in the presence of AA. Voltammetric techniques separated the anodic peaks of FA and UA with activation overpotential, and the interference from AA was effectively excluded from FA and UA determination. The differential pulse voltammetry (DPV) data showed that the obtained anodic peak currents were linearly proportional to concentration in the range of 1-1000  $\mu$ M with a detection limit (S/N = 3) of 0.8  $\mu$ M for FA and in the range of 0.1-500  $\mu$ M with a detection limit of 0.07  $\mu$ M for UA. It also presented superior reproducibility and long-term stability, as well as high selectivity. Moreover, the proposed sensor was successfully employed for the determination of FA and UA in spiked human urine samples with satisfactory results.

---

**Keywords:** Folic acid; Simultaneous determination; Poly(3,4-ethylenedioxythiophene); Single-walled carbon nanotubes; Sensor

## 1. INTRODUCTION

Folic acid (FA) is water-soluble of vitamin B group (VB9). It exists in the kidneys and livers of animals, plants, mushrooms and algae [1]. FA is an important substance for keeping activity and health

of living beings and is essential for cell growth and division in the human body. It participates in lots of bodily reactions and mainly in synthesis of nucleic acid and some important substances [2], and promotes the synthesis of protein from amino acid. Deficiency of FA causes high homotype cysteine acidemia, psychosis, devolution of mentality, and anaemia, and it is thought to increase the likelihood of heart attack and stroke [3]. As a consequence, it is necessary to quantify FA with reliable results.

As we known, uric acid (UA) is the primary final product of purine metabolism in the human body, and is excreted via urine [4]. It is of biomedical significance, and plays determining roles not only in human metabolism but also in the central nervous and renal systems. Abnormal levels of UA are symptoms of several diseases such as gout, hyperuricaemia and Lesch-Nyhan syndrome. UA is also a risk factor for leukemia, pneumonia and cardiovascular disease [5,6]. In addition, numerous reports have shown FA and UA usually co-exist biological systems and that they influence each other in their respective activities [7,8]. Therefore, investigation of neurological behavior and also simultaneous determination of FA and UA is of great importance for the elucidation of their precise physiological functions. Due to interesting electrochemical properties of FA and UA, application of the modified electrodes is considered as the common routes in this area. However, ascorbic acid (AA) is always coexisting with FA and UA in the extra cellular fluid of the central nervous system and serum. Therefore, simultaneous determination of FA and UA in the presence of AA is an important issue not only in diagnostic and pathological research but also in the field of biomedical chemistry. The electrochemical response of AA will certainly interfere in the detection of FA and UA under coexistence of AA on conventional electrodes. To resolve this problem, various chemical modification of electrode surface have been made for the determination of FA and UA in the presence of AA.

In the recent years, many of the studies focused on substituted polythiophene derivatives [9], and among others poly(3,4-ethylenedioxythiophene) (PEDOT) electrosynthesized either in organic or in aqueous media, has the advantage of providing very stable and highly conductive films [10-12]. This polymer possesses many favourable properties such as high conductivity, good biocompatibility, band gap width, excellent stability or optical transparency in its conducting state, as well as an environment-friendly feature [13-15]. Owing to these properties, it exhibits promising potential applications in various fields, such as electro-chromic devices, anti-static coatings, capacitors and fuel cells [16]. In addition, PEDOT has received particular attention for the electroanalytical application, e.g., detection of chemical [17] and biomolecules such as NADH [18], ascorbic acid [19] and cysteine [20], etc. due to retaining of its electroactivity for wide range of pH. Recently, the developments in nano-structured conducting polymers and polymer nanocomposites have large impact on electrocatalysis research and sensor applications [21]. Thus interest has been shown on the synthesis of carbon-based nanomaterials/PEDOT composites that exhibit unique properties of both individual components in a synergistic manner. Carbon nanotubes (CNTs), categorized as multi-walled carbon nanotubes (MWCNTs) and single walled carbon nanotubes (SWCNT), have generated a considerable interest since being discovered due to their excellent electrical conductivity, chemical stability, high surface area and high mechanical strength [22]. Consequently, CNTs have been used as an electrode material or modifier to promote electron transfer reactions between biomolecules and the underlying electrodes [23]. For these reasons, CNTs have the ability to compound with PEDOT to increase the mechanical properties of polymer and enhance the electrical characteristics by facilitating the charge-

transfer processes between the two components when used as electrodes for constructing of efficient electrochemical sensors. To the best of our knowledge, there is few article reported the simultaneous electroanalytical determination of FA and UA by using conducting polymer PEDOT nanocomposites.

The aim of this study was to combine the properties of conducting polymers and  $\beta$ -CD-functionalized SWCNT ( $\beta$ -CD-SWCNT) to prepare a composite that can be used for simultaneous determination folic acid and uric acid under coexistence of ascorbic acid. During the synthesis process,  $\beta$ -CD not only acts as dispersant and stabilizer for SWCNT, but also has the function of detection signal modification. The PEDOT film plays an important role in improving the electrical conductivity and the stability of the composite on the modified GCE. Compared with bare GCE, PEDOT/GCE and  $\beta$ -CD-SWCNT/GCE, the proposing PEDOT/ $\beta$ -CD-SWCNT composite reveals remarkably enhanced electrocatalytic activity towards FA, UA and AA significantly. When applied to simultaneous determination of FA and UA in the presence of AA by DPV, the modified electrode exhibited well-separated peaks and low detection limits. As the superduper performance, the sensor was successfully evaluated in human urine samples with satisfactory results.

## 2. MATERIALS AND METHODS

### 2.1. Chemicals and reagents

3,4-ethylenedioxythiophene (EDOT) was purchased from Sigma-Aldrich (USA). SWCNT suspension was purchased from Chengdu Institute of Organic Chemistry, Chinese Academy of Sciences (SWCNT content 1 wt%, diameter 1-2 nm, length 5-30  $\mu$ m).  $\beta$ -cyclodextrin ( $\beta$ -CD), lithium perchlorate trihydrate ( $\text{LiClO}_4$ ), disodium hydrogen phosphate dodecahydrate ( $\text{Na}_2\text{HPO}_4$ ), and sodium dihydrogen phosphate dehydrate ( $\text{NaH}_2\text{PO}_4$ ) were obtained from Sinopharm chemical reagent Co. Ltd. FA, UA and AA were purchased from Bio Basic Inc. FA and UA stock solution were prepared with diluted NaOH aqueous solution. All the used reagents were analytical grade, and used as received without further purification. All solutions were prepared using deionized distilled water as the solvents.

### 2.2. Apparatus

All electrochemical experiments were performed with a CHI 660D electrochemical workstation (CH Instrument Company, Shanghai, China), with a conventional three-electrode cell system, at room temperature. Inert atmosphere was set by passing  $\text{N}_2$  over the solution during the experiments. The working electrode was a modified glassy carbon electrode (3 mm in diameter), the auxiliary and reference electrodes were platinum wire and saturated calomel electrode (SCE) respectively. The pH value was measured with a Delta 320 pH meter. The infrared (IR) spectra were recorded with an Bruker Vertex 70 Fourier spectrophotometer (Netherlands).

### 2.3. Preparation of the electrodes

The  $\beta$ -CD functionalized SWCNT suspension ( $2 \text{ mg mL}^{-1}$ ) was prepared by dispersing SWCNT in 2 wt%  $\beta$ -CD by sonicating for about 2 hours until a homogeneous sol was obtained.

Before modification, GCE was polished to a mirror-like surface with  $0.05 \mu\text{m Al}_2\text{O}_3$  slurry, then rinsed with water, ultrasonicated in ethanol and doubly distilled water for 5 min, respectively. Subsequently, an aliquot of  $5.0 \mu\text{L}$   $\beta$ -CD-SWCNT suspension was scrupulously dropped onto the surface of the GCE and dried under an IR lamp for 1 h. Then the PEDOT was deposited using chronoamperometry under the potential of 1.1 V for 90 s by immersing the  $\beta$ -CD-SWCNT/GCE in aqueous solution containing 0.01 M EDOT and 0.02 M  $\text{LiClO}_4$ . The obtained PEDOT/ $\beta$ -CD-SWCNT/GCE was washed repeatedly with double-distilled deionized water to remove the electrolyte and monomer from electrode surface. For comparison, PEDOT/GCE, SWCNT/GCE,  $\beta$ -CD-SWCNT/GCE and PEDOT-SWCNT/GCE were also prepared in a similar procedure.

## 3. RESULTS AND DISCUSSION

### 3.1. FT-IR spectroscopic analysis of the PEDOT/ $\beta$ -CD-SWCNT composite

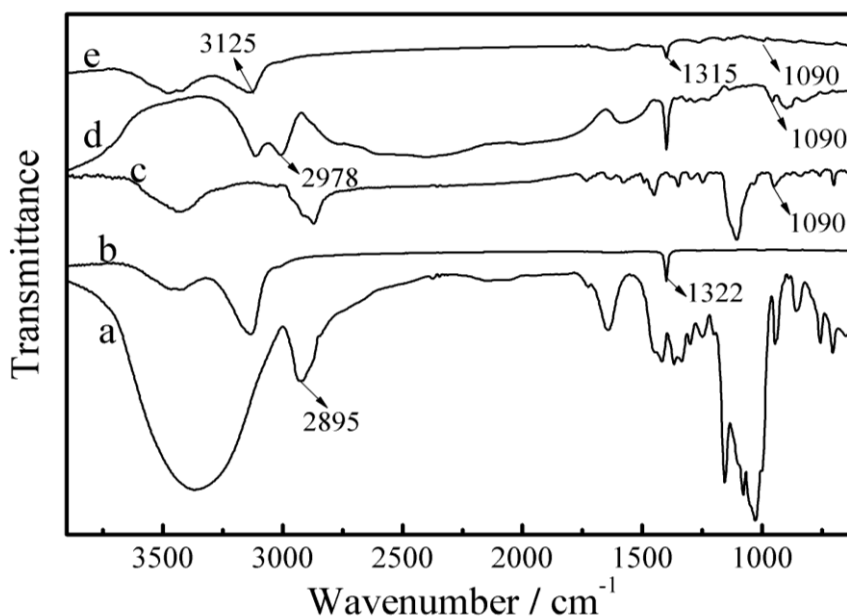


**Figure 1.** FT-IR of (a)  $\beta$ -CD, (b) PEDOT, (c) SWCNT, (d)  $\beta$ -CD-SWCNT and (e) PEDOT/ $\beta$ -CD-SWCNT films.

In order to confirm the formation of  $\beta$ -CD (a), PEDOT (b), SWCNT (c),  $\beta$ -CD-SWCNT (d) and PEDOT/ $\beta$ -CD-SWCNT (e) on the GCE, the technique of FT-IR was employed. As shown in Fig. 1,  $\beta$ -CD had a defined peak at  $2895 \text{ cm}^{-1}$ , which was assigned to the symmetric C-H stretching

vibration of the alkyl groups [24]. As for PEDOT (curve b), the band appeared at  $1322\text{ cm}^{-1}$  was assigned to the absorption of polymer backbone. SWCNT (curve c) presented absorption peak at  $1090\text{ cm}^{-1}$ , this could be ascribed to the stretching vibrations of C-OH [25]. As for the  $\beta$ -CD-SWCNT film (curve d), two absorption peaks are observed around  $2978$  and  $1090\text{ cm}^{-1}$ , respectively, and these peaks slightly shifted, which demonstrated that the  $\beta$ -CD had uniformly dispersed on the surface of SWCNT. When PEDOT and  $\beta$ -CD-SWCNT formed composite film (curve e), the IR spectrum combined the typical absorption peaks of PEDOT and  $\beta$ -CD-SWCNT. And the peak of PEDOT at  $1322\text{ cm}^{-1}$  shifted to  $1315\text{ cm}^{-1}$ , which was related to the interaction between PEDOT and  $\beta$ -CD-SWCNT [26]. Therefore, these results demonstrated PEDOT/ $\beta$ -CD-SWCNT had been successfully prepared.

### 3.2. Characterization the interface of the modified GCE with cyclic voltammogram and electrochemical impedance spectroscopy

$\text{Fe}(\text{CN})_6^{3-/4-}$ , as an electrochemical probe, is usually used to evaluate the electrochemical properties of the electrode. Fig. 2A shows the cyclic voltammograms (CVs) of differently modified electrodes in  $5.0\text{ mM Fe}(\text{CN})_6^{3-/4-}$  (1:1) containing  $0.1\text{ M KCl}$  at  $100\text{ mV s}^{-1}$ . The bare GCE (curve a) showed a pair of quasi-reversible peaks. The redox peak current decreased obviously after the  $\beta$ -CD deposition onto the bare GCE surface (curve b), which can be attributed to the poor electrical conductivity of  $\beta$ -CD. An increase in peak current was observed when SWCNT was covered onto the electrode (curve c), indicating that the electron transfer is quicker at  $\beta$ -CD-SWCNT/GCE. The peak current further increased again (curve d), when PEDOT was attached to the  $\beta$ -CD-SWCNT film-coated electrode surface, which may be attributed to the great capacitance of PEDOT.

Electrochemical impedance spectroscopy (EIS) can reveal the interfacial changes due to the surface modification of electrodes [27]. The semicircle diameter at high frequencies corresponds to the electron-transfer resistance ( $R_{et}$ ), and the linear portion at low frequencies may be attributed to diffusion process. Nyquist plots of the bare GCE (curve a),  $\beta$ -CD (curve b),  $\beta$ -CD-SWCNT (curve c) and PEDOT/ $\beta$ -CD-SWCNT (curve d) modified GCE were shown in Fig.2B. The curve a corresponding to bare GCE displayed a big well defined semicircle, the electron-transfer resistance ( $R_{ct}$ ) can be estimated to be  $750\ \Omega$ . The  $R_{ct}$  of the  $\beta$ -CD modified GCE (curve b) was about 1.5 times larger than that of the bare GCE, indicating that  $\beta$ -CD blocks electron transfer to some extent. For the  $\beta$ -CD-SWCNT/GCE (curve c), the  $R_{ct}$  decreases dramatically, the reason was that SWCNT can act as effective electron conduction pathway between the electrode and electrolyte. When PEDOT was deposited on the  $\beta$ -CD-SWCNT/GCE (curve d), the  $R_{ct}$  decreased to low levels. This result was due to that PEDOT could enhance the electroactive surface area and electronic conductivity of PEDOT/ $\beta$ -CD-SWCNT composite film.

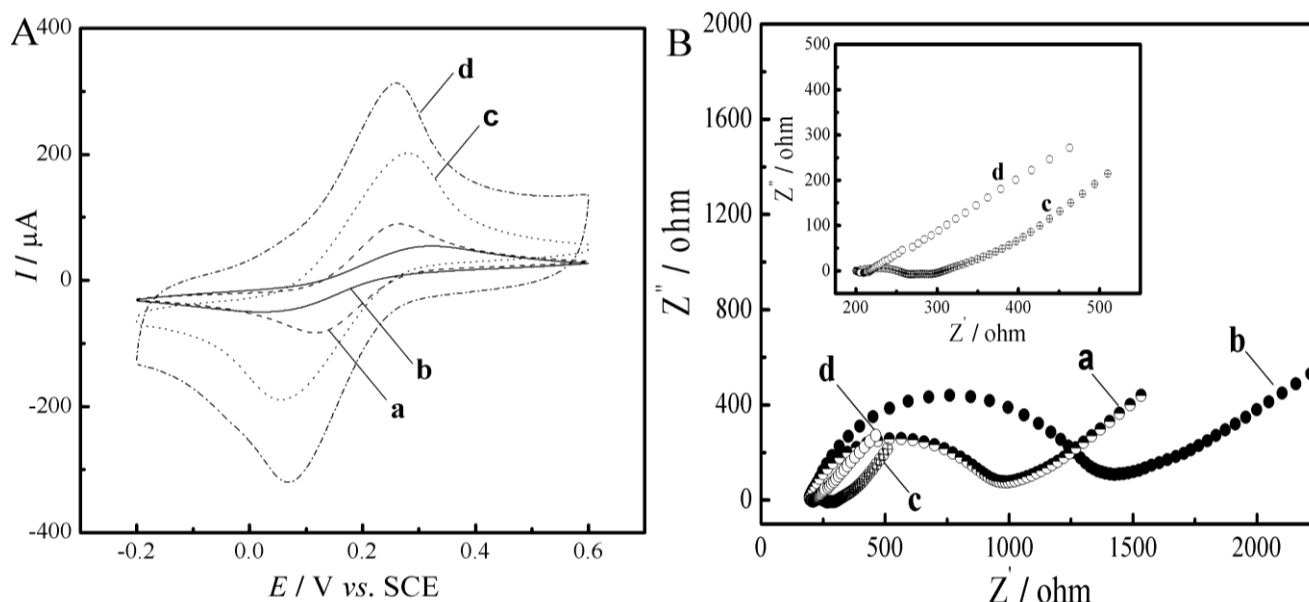


**Figure 2.** (A) Cyclic voltammograms of (a) bare GCE, (b)  $\beta$ -CD/GCE, (c)  $\beta$ -CD-SWCNT/GCE and (d) PEDOT/ $\beta$ -CD-SWCNT/GCE in 5.0 mM  $\text{Fe}(\text{CN})_6^{3-/4-}$  (1:1) containing 0.1 M KCl. Scan rate:  $50 \text{ mV s}^{-1}$ ; (B) Nyquist plots of (a) bare GCE, (b)  $\beta$ -CD/GCE, (c)  $\beta$ -CD-SWCNT/GCE and (d) PEDOT/ $\beta$ -CD-SWCNT/GCE in 5.0 mM  $\text{Fe}(\text{CN})_6^{3-/4-}$  (1:1) containing 0.1 M KCl. Frequency range: 0.1 to 104 Hz. (Inset) Nyquist plots of (c)  $\beta$ -CD-SWCNT /GCE and (d) PEDOT/ $\beta$ -CD-SWCNT/GCE.

### 3.3. Electrochemical behaviors of FA, UA and AA mixture by CV at different modified electrodes

The electrocatalytic oxidation of FA, UA and AA mixture at bare and different modified electrodes have been investigated by cyclic voltammetry. Fig.3. depicted the CV comparison of the bare GCE (a), PEDOT/GCE (b), SWCNT/GCE (c),  $\beta$ -CD-SWCNT/GCE (d), PEDOT-SWCNT/GCE (e) and PEDOT/ $\beta$ -CD-SWCNT/GCE (f) in deoxygenating PBS solution containing 0.3 mM FA, 0.2 mM UA and 0.35 mM AA. For the bare GCE, a small oxidation peak of FA was at 0.85 V, and at 0.55 V a rather broad oxidation peak was observed which was derived from the simultaneous oxidation of UA and AA [28]. Obviously, the individual UA and AA cannot be distinguished. However, three well-resolved anodic peaks and higher voltammetric current are found at PEDOT/GCE, SWCNT/GCE and  $\beta$ -CD-SWCNT/GCE relative to those at the bare GCE, indicating a favorable catalytic activity of PEDOT, SWCNT and  $\beta$ -CD-SWCNT toward the oxidation of FA, UA and AA. It also can be seen that the oxidation peaks of FA, UA and AA were superior resolved and the voltammetric signals showed considerable enhancements at  $\beta$ -CD-SWCNT/GCE in comparison with that at SWCNT/GCE. The reason may be discussed as two aspects: firstly, SWCNT was effectively dispersed by  $\beta$ -CD, which could improve the mechanical, electrical and catalytic properties of SWCNT; secondly,  $\beta$ -CD showed the high supramolecular recognition capability toward FA, UA and AA. Particularly, PEDOT/ $\beta$ -CD-SWCNT/GCE can be found its obviously higher electrocatalytic oxidation current for FA, UA, and AA mixture. Such excellent catalytic activity of PEDOT/ $\beta$ -CD-SWCNT might be attributed to the

synergistic reaction of PEDOT and  $\beta$ -CD-SWCNT. PEDOT on the surface of  $\beta$ -CD-SWCNT with a high density would provide more active sites for the catalytic redox reaction and greatly increase the electrocatalytic activity. As the examined results, PEDOT/ $\beta$ -CD-SWCNT/GCE can be a good choice to simultaneously determine FA and UA in the presence of AA (depicted in Scheme 1).

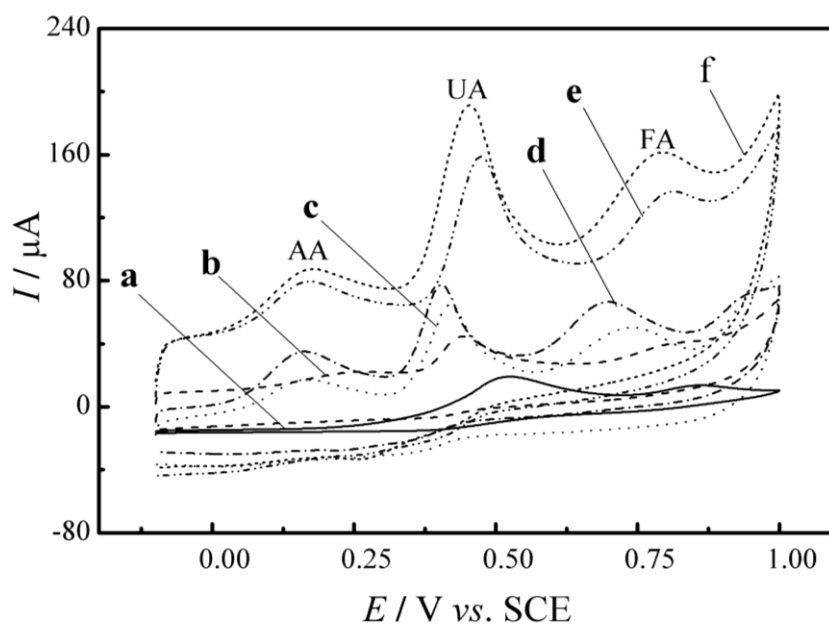
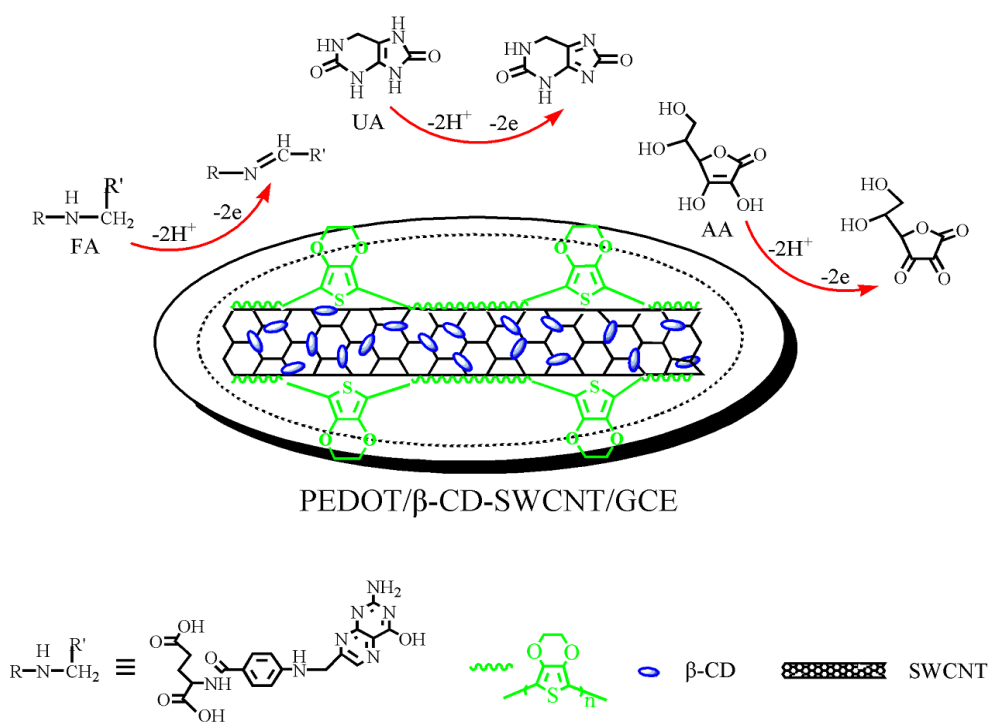


**Figure 3.** Cyclic voltammograms of (a) bare GCE, (b) PEDOT/GCE, (c) SWCNT/GCE, (d)  $\beta$ -CD-SWCNT/GCE, (e) PEDOT-SWCNT/GCE and (f) PEDOT/ $\beta$ -CD-SWCNT/GCE in the absence and presence 0.3 mM FA, 0.2 mM UA and 0.35 mM AA in 0.1 M PBS (pH 5.0). Scan rate:  $50 \text{ mV s}^{-1}$ .



**Scheme 1.** The oxidation mechanism of FA, UA and AA at the PEDOT/ $\beta$ -CD-SWCNT/GCE.

### 3.4. Effect of solution pH

In most case, the solution pH was an important influence factor to the electrochemical reaction. The effect of solution pH on the electrocatalytic oxidation of FA and UA under coexistence of AA at the PEDOT/ $\beta$ -CD-SWCNT/GCE was investigated by DPV in the pH range from 4.0 to 8.0 at a scan rate of  $50 \text{ mV s}^{-1}$  (Fig.4.). The results showed that with the increase of solution pH the oxidation peak potentials of the two molecules shift to negative values. The peak potential of FA was proportional to pH with the linear regression equations  $E_{\text{pa}} (\text{V}) = 0.8714 - 0.0258 \text{ pH}$  ( $R^2 = 0.9875$ ), which indicated that in the electrode reaction the number of transferred electrons is double of proton number, implying that two electrons with one proton transfer is involved in the oxidation process of FA. This was agreement with that reported in literature [29]. The peak potential of UA was proportional to pH with the linear regression equations  $E_{\text{pa}} (\text{V}) = 0.6592 - 0.0480 \text{ pH}$  ( $R^2 = 0.9927$ ). It demonstrated that an equal number of electrons and protons involved in the electrochemical oxidations of UA.

Moreover, it can be informed that the anodic peak current of FA reached a maximum at pH 5.0, and then decreased gradually with increase of pH value. On the contrast, the oxidation peak currents of UA gradually decreased with the solution pH range from 5.0 to 8.0. The results indicated that the electrostatic interaction between UA and modified electrode played the leading role. Considering the separation effect and detection sensitivity, the buffer solution pH of 5.0 was selected as the optimum value in the following measurements.

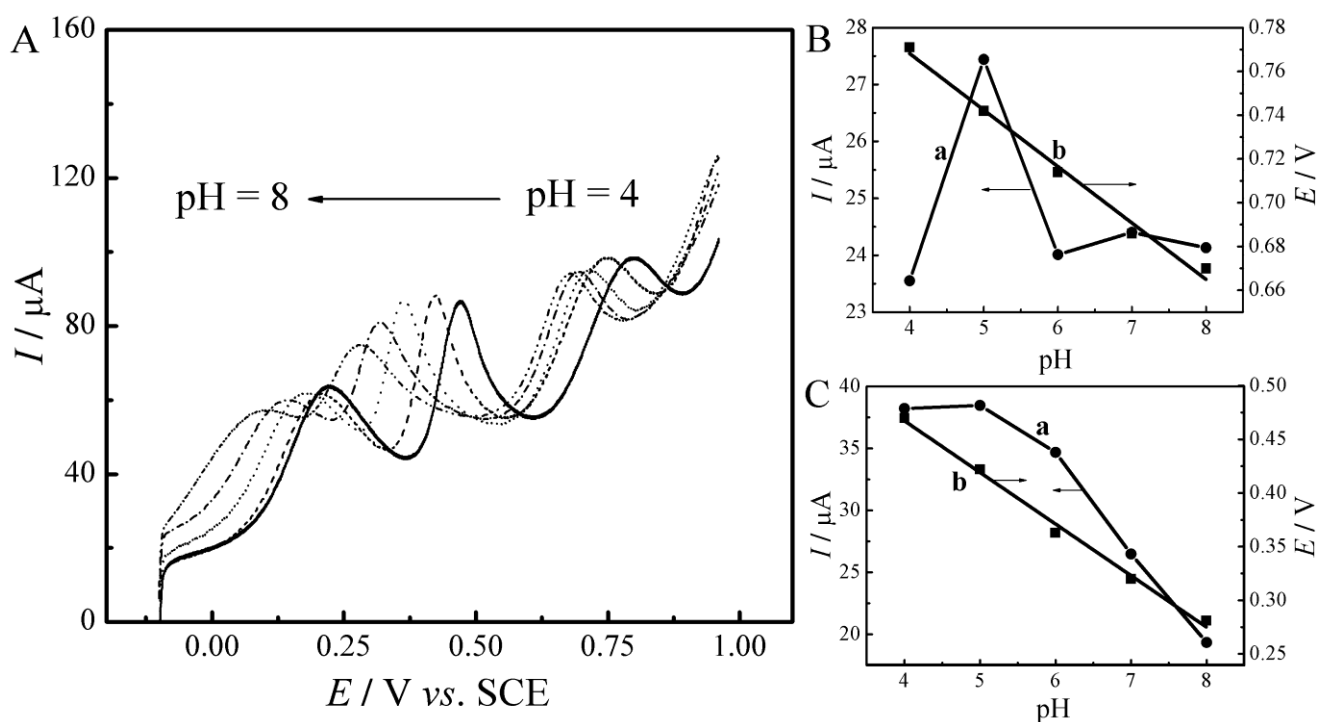


**Figure 4.** (A) Differential pulse voltammeters of PEDOT/ $\beta$ -CD-SWCNT/GCE in PBS at different pHs from 4 to 8 in the presence of 0.2 mM FA, 0.3 mM UA and 0.5 mM AA; (B) The peak current (a) and peak potential (b) of FA with solution pH; (C) The peak current (a) and peak potential (b) of UA with solution pH.

### 3.5. Effect of scan rate

To elucidate the process kinetic of FA and UA in the presence of AA electro-oxidation at electrode surface, CVs of different scan rates on the peak currents at the PEDOT/ $\beta$ -CD-SWCNT/GCE were recorded in Fig.5. The oxidation peak currents for FA and UA increased with increasing the sweep rates, while their oxidation peak potentials gradually shifted to positive values, suggesting the electron transfer was quasi-reversible. Plots of the anodic peak currents intensified linearly as the scanning rate increased from 20 to 300  $\text{mV s}^{-1}$ , which displayed the electrode reactions of FA and UA were adsorption-controlled processes, according to the following equations:  $I_{\text{pa}} (\mu\text{A}) = -28.00 + 5.48 v (\text{V s}^{-1})$  and  $I_{\text{pc}} (\mu\text{A}) = 655.93 + 10.43 v (\text{V s}^{-1})$  with the correlation coefficients ( $R^2$ ) of 0.9575 and 0.9946, respectively. This result was well consistent with other previous studies [30].

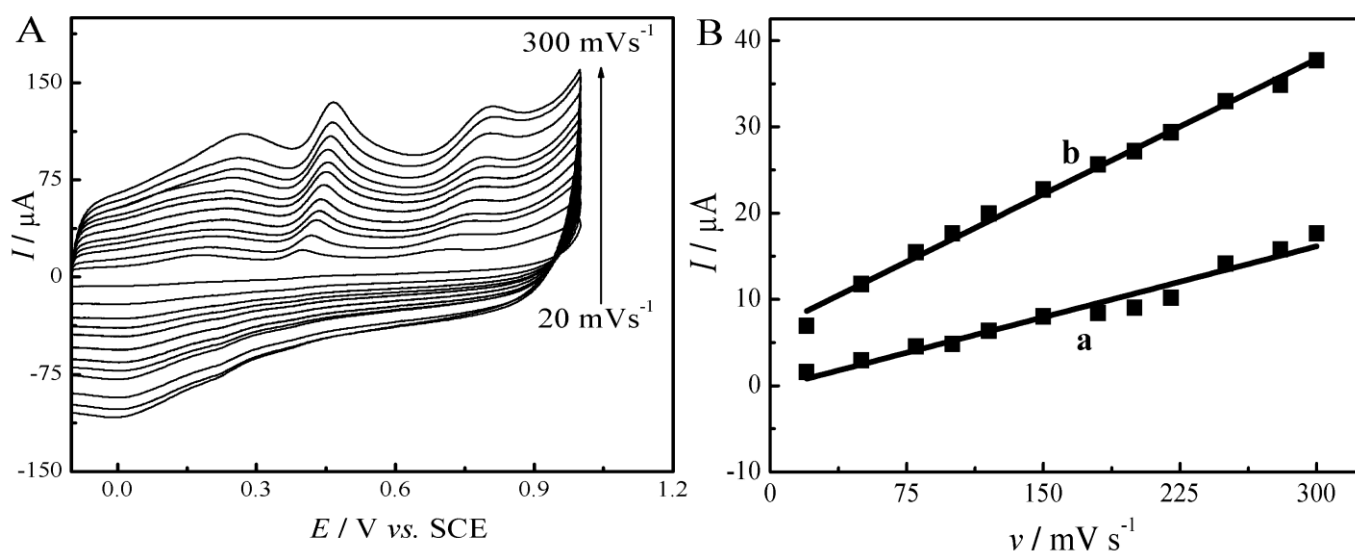


**Figure 5.** (A) Cyclic voltammograms of 0.6 mM FA, 0.4 mM UA and 0.8 mM AA at different scan rates. The scan rate (from bottom to top): 20, 50, 80, 100, 120, 150, 180, 200, 220, 250 and 300  $\text{mV s}^{-1}$ ; (B) The plot of the peak currents (a) UA and (b) FA vs. scan rate.

### 3.6. Simultaneous determination of FA and UA at PEDOT/ $\beta$ -CD-SWCNT/GCE

Since DPV has much higher current sensitivity and selectivity than CV does, then it was used to estimate the linear range, detection limit, and simultaneous determination of FA and UA in the presence of AA under the optimized experimental conditions. As is shown in Fig.6., DPVs for the oxidation of different concentrations of FA in the presence of 8  $\mu\text{M}$  UA and 200  $\mu\text{M}$  AA at the PEDOT/ $\beta$ -CD-SWCNT/GCE were obtained. An increase in the peak current of UA is observed with increasing FA concentration and the voltammetric peak of UA is almost unchanged during the oxidation of FA. The plot of peak currents versus FA concentration was constituted of a wide linear segment (1-1000  $\mu\text{M}$ ) and low detection limit (0.8  $\mu\text{M}$ ), with correlation coefficient of 0.9986. Also, the various concentrations of UA in the coexistence of 100  $\mu\text{M}$  FA and 200  $\mu\text{M}$  AA exhibited excellent DPV responses although that of the FA remains almost constant (Fig.7.). The modified

electrode had linear current-to-concentration relationship for UA in the broad range from 0.1  $\mu\text{M}$  to 500  $\mu\text{M}$  with a correlation coefficient of 0.9957. From the analysis of data, we estimate that the lower limit of detection of UA was approximately 0.07  $\mu\text{M}$ . Table 1 gives the comparison of some of the analytical parameters obtained for FA and UA in this study with other previous literatures. It can be observed that the proposed electrode is superior in some cases, as compared to the previously reported modified electrodes.

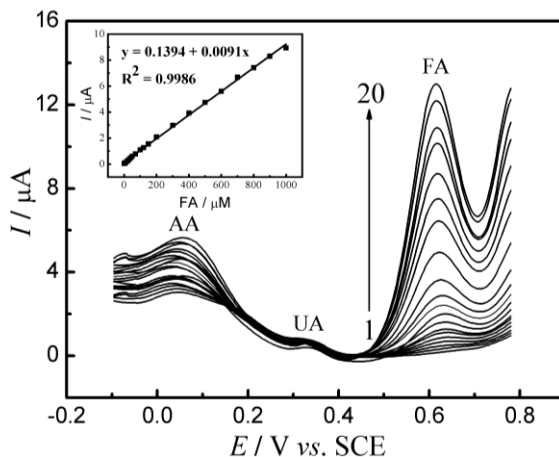


**Figure 6.** Differential pulse voltammetry profiles at PEDOT/ $\beta$ -CD-SWCNT/GCE in PBS (pH 5.0) containing 200  $\mu\text{M}$  AA, 8  $\mu\text{M}$  UA and different concentrations of FA from 1 to 20 (Curve 1 to 20 is corresponding to 1, 5, 10, 20, 30, 40, 50, 70, 100, 120, 150, 200, 300, 400, 500, 600, 700, 800, 900 and 1000  $\mu\text{M}$ ). (Inset) Plots of the oxidation peak current as a function of FA concentrations.

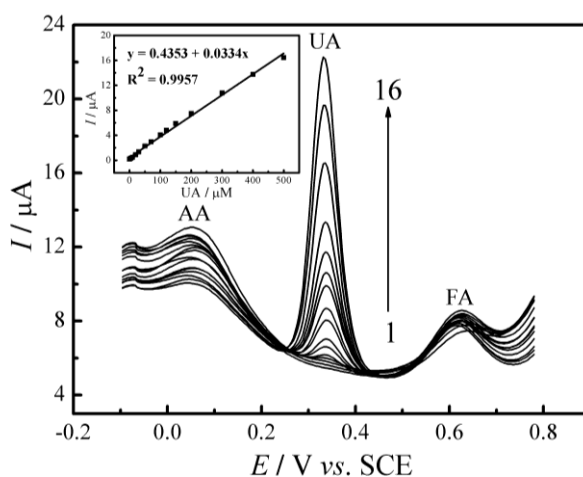


**Figure 7.** Differential pulse voltammetry profiles at PEDOT/ $\beta$ -CD-SWCNT/GCE in PBS (pH 5.0) containing 200  $\mu\text{M}$  AA, 100  $\mu\text{M}$  FA and different concentrations of UA from 1 to 16 (Curve 1 to 16 is corresponding to 0.1, 0.5, 1, 5, 10, 20, 30, 50, 70, 100, 120, 150, 200, 300, 400 and 500  $\mu\text{M}$ ). (Inset) Plots of the oxidation peak currents as a function of UA concentrations.

**Table 1.** The comparison of PEDOT/ $\beta$ -CD-SWCNT/GCE with other FA and UA sensors.

Electrode name	Method	Detection limit ( $\mu$ M)		Linear range ( $\mu$ M)		Ref
		FA	UA	FA	UA	
PBNBH/CNTPE	DPV	11.0	8.8	15-800	25-750	31
PBNBH-TONPs/CPE	DPV	-	-	14-230	100-140	32
Chloranil/CNTPE	DPV	-	-	15-900	10-1100	33
ZONPs/CPE	DPV	9.86	-	20-2500	-	34
RGO-AuNPs-CSHMs/GCE	DPV	-	0.3	-	1-300	35
PEDOT/ $\beta$ -CD-SWCNT/GCE	DPV	0.8	0.07	1-1000	0.1-500	This work

PBNBH : 2,2-(1,3-propanediylbisnitrilo-ethylidene) bis-hydroquinone

TONPs : TiO<sub>2</sub> nanoparticles

ZONPs : ZnO<sub>2</sub> nanoparticles

CSHMs : chitosan/silica solgel hybrid membranes

### 3.7. Anti-interference ability and stability

The anti-interference ability of the PEDOT/ $\beta$ -CD-SWCNT/GCE was tested towards the detection of  $5 \times 10^{-5}$  M FA or UA in the presence of various common ions such as  $1 \times 10^{-2}$  M for Na<sup>+</sup>, Cl<sup>-</sup>, K<sup>+</sup>, Mg<sup>2+</sup>, SO<sub>4</sub><sup>2-</sup>, Ca<sup>2+</sup>, CO<sub>3</sub><sup>2-</sup> and some physiological interferents for instance  $5 \times 10^{-3}$  M of L-lysine, glucose, L-asparagines, glutamic acid, glycine, L-cystine, L-cysteine and NADH by DPV method. As a satisfying result, no obvious change in the oxidation peak potentials and currents of FA and UA were observed in the determination. It also indicated that the present modified electrode was highly selective towards the detection of these analytes.

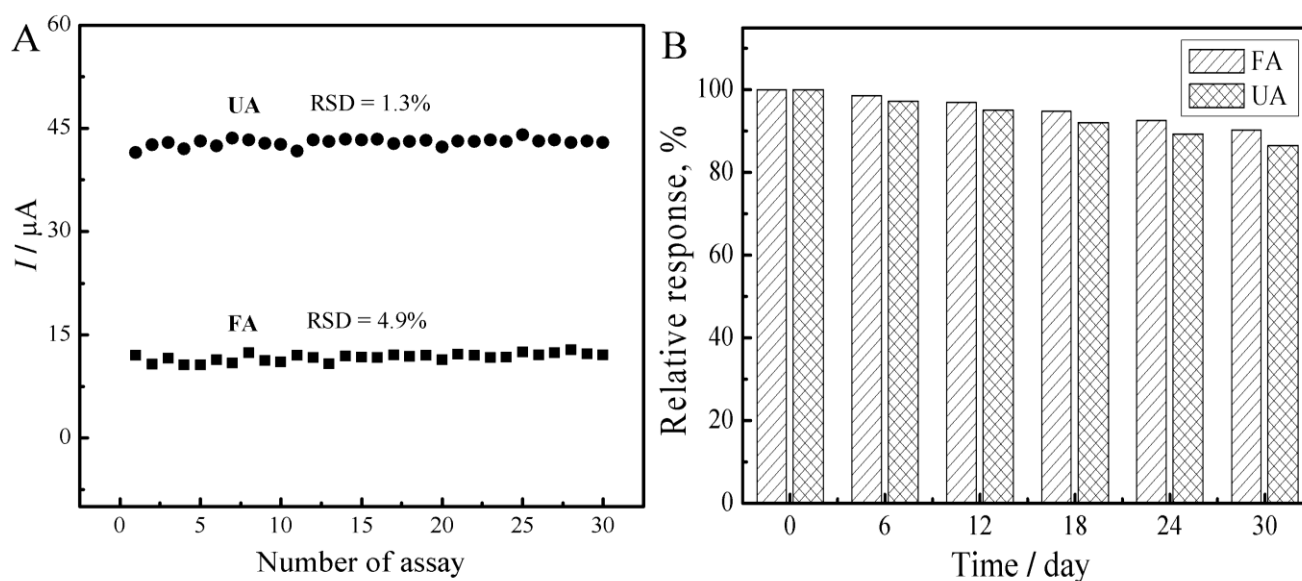


**Figure 8.** (A) Operational stability and (B) Long-term storage stability of the sensor.

Stability is another advantage of the PEDOT/ $\beta$ -CD-SWCNT/GCE, which was tested by measuring the response current decay during repetitive CV cycling and long-term storage at room temperature. Fig.8A shows repetitive measurements examined in PBS containing 0.5 mM FA and 0.25 mM UA with 30 successive determinations using the same modified electrode. The average peak currents for two biomolecules were 13.15  $\mu$ A with the relative standard deviation (RSD) of 4.9% and 43.24  $\mu$ A with the RSD of 1.3%, respectively. The long-term stability of the sensor was also investigated in the same solution. The peak potential for FA and UA oxidation was unchanged and the current response signals decreased about 1.5% (FA) and 2.4% (UA) of its initial response during the first 6 days. From Fig.8B it also can see the current response of the sensor decreased gradually and retained 91% and 86% of its original activity after a month and displayed excellent response to FA and UA, respectively. This achievement manifested that PEDOT/ $\beta$ -CD-SWCNT nanocomposite film had ability to prevent the electrode from fouling by the oxidation product and to be very stable on the electrode surface for a long time.

### 3.8. Real sample analysis

Finally, to verify its workability, the modified electrode was applied to the determination of FA and UA in human urine sample. The urine sample was diluted 500 times with 0.10 M pH 5.0 PBS before the measurement to fit the calibration curve. Both biomolecules content in urine sample was determined by the standard addition method to prevent any matrix influence. This proposed electrode system gave rise to better recoveries (Table 2) for the quantification of spiked two drugs using DPV technique under optimized conditions. The results were acceptable, showing that the sensor can be used efficiently for the determination of FA and UA in sample analysis.

**Table 2.** Determination and recovery results of FA and AA in human urine sample by PEDOT/ $\beta$ -CD-SWCNT/GCE.

Sample	Added ( $\mu$ M)	Found ( $\mu$ M)	Recovery (%)	RSD (%)
	-	< DL	-	-
1	10.0	10.20 $\pm$ 0.24	102.0	3.01
FA	2	40.32 $\pm$ 0.55	108.0	1.72
	3	69.67 $\pm$ 0.78	99.5	1.27
	-	< DL	-	-
1	5.0	5.17 $\pm$ 0.11	103.4	2.76
UA	2	20.17 $\pm$ 0.82	108.5	3.89
	3	49.51 $\pm$ 0.75	99.0	1.52

## 4. CONCLUSIONS

In summary, simultaneous trace determination of FA and UA under coexistence of AA was achieved by using PEDOT/ $\beta$ -CD-SWCNT/GCE. Attributing to the increase in electrical conductivity

and the large effective surface area of PEDOT/ $\beta$ -CD-SWCNT film, the modified electrode exhibits an excellent electrocatalytic activity towards the oxidation of FA, UA and AA. As the PEDOT/ $\beta$ -CD-SWCNT/GCE provides excellent sensitivity, selectivity and stability to determine of FA and UA in the presence of AA, the proposed sensor was applied to the determination of FA and UA in spiked human urine samples, and satisfying results were achieved. The simple fabrication procedure, wide linear range, low detection limit, high stability and good reproducibility for repeated determination suggest that this electrode will be a good and attractive candidate for practical applications.

#### ACKNOWLEDGEMENTS

This work was supported by the National Natural Science Foundation of China (50963002, 51073074, 51272906, 51263010), Natural Science Foundation of Jiangxi Province (2010GZH0041, 20122BAB213007), Jiangxi Provincial Department of Education (GJJ11590, GJJ10678) and State Key Laboratory of Chemical Biosensing & Chemometrics (201108).

#### References

1. S. Cakir, E. Bicer and O. Cakir, *J. Inorg. Biochem*, 11 (1999) 249
2. H.X. Guo, Y.Q. Li, L.F. Fan, X.Q. Wu and M.D. Guo, *Electrochim. Acta*, 51 (2006) 6230
3. D. Hoegger, P. Morier, C. Vollet, D. Heini, F. Reymond and J.S. Rossier, *Anal. Bioanal. Chem*, 387 (2007) 267
4. S.H. Huang, Y.C. Shih, C.Y. Wu and C.J. Yuan, *Biosens. Bioelectron*, 19 (2004) 1627
5. E. Miland and A.J. Miranda Ordieres, *Talanta*, 43 (1996) 785
6. M.H. Alderman, *Curr. Opin. Pharmacol*, 2 (2002) 126
7. D. Hoegger, P. Morier, C. Vollet, D. Heini, F. Reymond and J.S. Rossier, *Anal. Bioanal. Chem*, 387 (2007) 267
8. S.L. Zhao, H.Y. Yuan, C. Xie and D. Xiao, *J. Chromatogr. A*, 1107 (2006) 290
9. R. D. McCullough, *Adv. Mater*, 10 (1998) 93
10. V. Vasantha and K. Phani, *J. Electroanal. Chem*, 520 (2002) 79
11. G. Li and P.G. Pickup, *Phys. Chem. Chem. Phys*, 2 (2000) 1255
12. V. Tsakova, S. Winkels and J.W. Schultze, *Electrochim. Acta*, 46 (2001) 759
13. G. Heywang and F. Jonas, *Adv. Mater*, 4 (1992) 116
14. Q. Pei, G. Zuccarello, M. Ahlskog and O. Inganas, *Polymer*, 35 (1994) 1347
15. C.Y. Lin, A. Balamurugan, Y.H. Lai and K.C. Ho, *Talanta*, 5 (2010) 1905
16. Z.Y. Guo, Y.C. Qiao, H. Liu, C.M. Ding, Y. Zhu, M.X. Wan and L. Jiang, *J. Mater. Chem*, 22 (2012) 17153
17. A. Balamurugan and S.M. Chen, *Electroanal*, 21 (2009) 1419
18. A. Balamurugan and S.M. Chen, *Sens. Actuator B: Chem*, 129 (2008) 850
19. S.S. Kumar, J. Mathiyarasu, K.L.N. Phani, Y.K. Jain and V. Yegnaraman, *Electroanal*, 17 (2005) 2281
20. W.Y. Su and S.H. Cheng, *Electrochem. Commun*, 10 (2008) 899
21. A.R. Tarushee and K. Devendra, *Sens. Actuator B: Chem*, 136 (2009) 275
22. S. Iijima, *Nature*, 354 (1991) 56
23. J. Wang and M. Musameh, *Anal. Chem*, 75 (2003) 2075
24. C.H. Xu, X.B. Wang, J.C. Wang, H.T. Hu and L. Wan, *Chem. Phys. Lett*, 498 (2010) 162
25. F. Xiao, C.P. Ruan, L.H. Liu, R. Yan, F.Q. Zhao and B.Z. Zeng, *Sens. Actuator B: Chem*, 134 (2008) 895

26. T. Fukushima, A. Kosaka, Y. Ishimura, T. Yamamoto, T. Takigawa, N. Ishii and T. Aida, *Science*, 300 (2003) 2072
27. E. Katz and I. Willner, *Electroanal*, 15 (2003) 913
28. Z.Q. Gao and H. Huang, *Chem. Commun*, 8 (1998) 2107
29. S.H. Wei, F.Q. Zhao, Z.Y. Xu and B.Z. Zeng, *Microchim. Acta*, 152 (2006) 285
30. A. Babaei and A.R. Taheri, *Sens. Actuator B: Chem*, 176 (2013) 543
31. H. Beitollahi, M.M. Ardakani, B. Ganjipour and H. Naeimi, *Biosens. Bioelectron*, 24 (2008) 362
32. M.M. Ardakani, R. Arazi and H. Naeimi, *Int. J. Electrochem. Sci*, 5 (2010) 1773
33. H. Yaghoobian, V.S. Nejad and S. Roodsaz, *Int. J. Electrochem. Sci*, 5 (2010) 1411
34. M. M. Ardakani, H. Beitollahi, M.K. Amini, F. Mirkhalaf and M.A. Alibeik, *Sens. Actuator B: Chem*, 151 (2010) 243
35. X. Liu, L.L. Xie and H.L. Li, *J. Electroanal. Chem*, 682 (2012) 158